Journal of the Serbian Chemical Society
JSCS-info@shd.org.rs • www.shd.org.rs/JSCS

J. Serb. Chem. Soc. *78* (11) 1655–1670 (2013)
JSCS–4525

UDC 615.211:546.41:577.112.02:
543.422.25:577.1:544
Original scientific paper

Halothane binds to druggable sites in the $[Ca^{2+}]_4$-calmodulin (CaM) complex, but does not inhibit $[Ca^{2+}]_4$-CaM activation of kinase

NENAD O. JURANIĆ[1]*, KEITH A. JONES[2], ALAN R. PENHEITER[1], THOMAS J. HOCK[2] and JOHN H. STREIFF[2]

[1]*Mayo College of Medicine at Rochester, U.S.A. and*
[2]*University of Alabama at Birmingham, U.S.A.*

(Received 23 May 2013)

Abstract: The mechanism(s) of volatile anesthetics (VAs) are poorly understood. High-resolution NMR spectroscopy was used to determine the structure of the halothane–$[Ca^{2+}]_4$-calmodulin ($[Ca^{2+}]_4$-CaM) complex, and it was found that halothane molecules bind in the druggable sites. Then it was examined whether VAs binding to druggable sites in calmodulin would affect the $[Ca^{2+}]_4$-CaM dependent activity of myosin light chain kinase. Fluorescence assays were used to determine that VA mediate $[Ca^{2+}]_4$-CaM activation of smooth-muscle-myosin-light-chain-kinase (smMLCK), but do not alter significantly the K_d of $[Ca^{2+}]_4$-CaM binding to skeletal-myosin-light-chain-kinase-peptide recognition sequence (skMLCKp). The results suggested that VAs do not alter $[Ca^{2+}]_4$-CaM dependent MLCK activity *via* direct interactions with $[Ca^{2+}]_4$-CaM.

Keywords: volatile anesthetic, calmodulin, halothane, drugs, protein structure.

INTRODUCTION

Volatile anesthetic (VA) drugs are used extensively with little knowledge of their cellular targets or mechanisms. The targets likely include proteins because anesthetic effects ultimately manifest as changes in protein function. This is further supported by the observation that the bioluminescent protein luciferase is inhibited *in vitro* by direct interaction with a variety of anesthetic agents.[1]

Calmodulin (CaM) is a ubiquitous Ca^{2+} second messenger that regulates many anesthetic sensitive systems. CaM has two EF hands, Ca^{2+}-binding domains that can bind up to 2 Ca^{2+} ions each. The EF hands are located at the N- and C- termini and are separated by a flexible central helix. The main difference between calcium-free CaM (apoCaM) and $[Ca^{2+}]_4$-CaM is the interhelical angle

* Corresponding author. E-mail: juranic.nenad@alumni.mayo.edu
doi: 10.2298/JSC130523090J

between the Ca^{2+} binding domains, which increases upon Ca^{2+} binding and exposes large hydrophobic pockets in each termini to the aqueous environment.[2] These hydrophobic pockets are critical for the interaction of $[Ca^{2+}]_4$-CaM with many proteins and hence the regulation of numerous enzymatic pathways. The Ca^{2+} dissociation constant (K_d) of $[Ca^{2+}]_4$-CaM is decreased by ligands, peptides, and proteins to the extent that they reduce the effective hydrophobic surface of $[Ca^{2+}]_4$-CaM exposed to an aqueous environment.[3] In other words, Ca^{2+} signaling through CaM is partially tuned by the target.

$[Ca^{2+}]_4$-CaM antagonists bind in the hydrophobic pockets of $[Ca^{2+}]_4$-CaM,[4] with a concomitant decrease in the Ca^{2+} K_d of $[Ca^{2+}]_4$-CaM,[5] and inhibition of $[Ca^{2+}]_4$-CaM activation of enzyme activity.[6] Short chain *n*-alcohols also bind to the hydrophobic pockets of $[Ca^{2+}]_4$-CaM,[7] and decrease the Ca^{2+} K_d of $[Ca^{2+}]_4$--CaM.[8]

It was found and verified that the VAs halothane and isoflurane decrease the Ca^{2+} K_d of $[Ca^{2+}]_4$-CaM.[9,10] It was shown that VAs bind to $[Ca^{2+}]_4$-CaM, but not to apoCaM.[10] This suggests that VAs bind to sites in $[Ca^{2+}]_4$-CaM that are either not present or not accessible in apoCaM. Together, these finding suggest that VAs bind to the hydrophobic pockets of $[Ca^{2+}]_4$-CaM. This was supported by docking studies that indicated that the VAs halothane, isoflurane, and sevoflurane bind within the hydrophobic pockets in both the N- and C-termini.[10,11] Thus, it was posited that VAs, as alcohols, would inhibit $[Ca^{2+}]_4$-CaM dependent enzymes and might directly antagonize $[Ca^{2+}]_4$-CaM.

The objective of this work was to verify that VAs bind to the hydrophobic pockets in $[Ca^{2+}]_4$-CaM and determine whether they antagonize the $[Ca^{2+}]_4$--CaM-dependent myosin light chain kinase (smMLCK) activity. This work is significant because it will test whether the effects of VAs on protein function could arise from low affinity ligand binding to druggable sites.

EXPERIMENTAL

Proteins and peptides

Human calmodulin cDNA was sub-cloned into the pET-15b expression vector (Novagen, San Diego, CA) using standard cloning techniques. CaM was overexpressed in BL21(DE3)-pLysS strain of *Escherichia coli* (Single Shot, Novagen, San Diego, CA). Uniform ^{13}C, ^{15}N enrichment was achieved by growing cells in Luria–Bertani medium and then inducing in minimal media containing ^{13}C-glucose and $^{15}NH_4Cl$ following established protocols.[12] Isotopically labeled and unlabeled CaM were purified using a slight modification to an existing procedure.[13] Thus, 5 mM $CaCl_2$ was added to the cleared cell lysate, which was loaded onto a phenyl-sepharose CL-4B column (Sigma, St. Louis, MO), and the CaM was eluted with 1 mM ethylene glycol tetraacetic acid (EGTA). The CaM fractions were further purified using a HiTrap Q column (Amersham Biosciences, Uppsala, Sweden) and a 0–1 M NaCl gradient. CaM was greater than 95 % pure, judging by SDS-gel electrophoresis with Coomassie Brilliant Blue staining. The identity of the CaM was confirmed by N-terminal sequencing as well as by LC–MS analysis of tryptic digests of labeled and unlabeled CaM. The molecular weight

and labeling efficiency (96 %) were verified by ESI-MS by direct infusion. Smooth muscle myosin light chain kinase (smMLCK) isoform 5 was prepared as previously described.[14]

Human MLC cDNA was sub-cloned into pET-15b expression vector (Novagen, San Diego, CA) using standard cloning techniques. MLC was overexpressed in BL21(DE3)-pLysS strain of *E. coli* (Single Shot, Novagen, San Diego, CA). The regulatory light chain (AL050318) was amplified from dT-primed cDNA derived from human lens epithelial cells using Fusion polymerase from New England Bio Labs. The primers used for amplification were Nde1 forward gccatatgtccagcaagcgggccaa and Spe1 reverse gaactagtctagtcgtctttatccttggcgcc. The amplified cDNA was cloned into a pET 15 B vector containing an N-terminal his tag linearized with Nde1 and Spe1 using standard cloning techniques. Recombinant clones were sequence verified. Protein expression was performed using Magic Media (Invitrogen). Briefly, an isolated clone was grown overnight in 50 ml Magic Media. The cells were pelleted by centrifugation at 5000*g* and lysed in Bug Buster media (Novagen). The inclusion bodies were collected by centrifugation and resuspended in 50 mM Tris–HCl (pH 8), 7 M urea, 250 mM NaCl, and 1 mM 2-mercaptoethanol. The solution was passed over a Ni-NTA column equilibrated in the same buffer. The protein was refolded on the column using a urea gradient (8 to 0 M) flowing at 0.2 ml min^{-1} for 16 h. The protein was eluted using a buffer containing 50 % glycerol, 50 mM Tris–HCl (pH 8), 250 mM imidazole, and 1 mM 2-mercaptoethanol. The MLC was judged greater than 90 % pure by SDS-PAGE with Coomassie Brilliant Blue staining.

The skeletal myosin light chain kinase peptide recognition sequence (skMLCKp) (biotin-CAAARWKKNFIAVSAANRFKKIS) was synthesized by Genetech, inc. (San Antonio, TX).

Lactate dehydrogenase, pyruvate kinase, phosphoenolpyruvate (PEP), NADH, and ATP were purchased from Sigma (St. Louis, MO).

NMR spectroscopy

Samples of 2mM [^{13}C,^{15}N]CaM, or 2mM [^{15}N]CaM, in aqueous solvent (95 % H_2O, 5 % D_2O), containing 100 mM KCl, 50 mM 3-morpholinopropane-1-sulfonic acid (MOPS, pH 7.2), 20 mM $CaCl_2$, 5 mM MgCl, 1 mM EDTA, were equilibrated with halothane to various mole ratios. It was possible to achieve up to about 1:70 CaM:halothane ratio, as determined by proton NMR. For structure determination the samples with 1:10 CaM:halothane ratio were used. Preparation of samples in the oriented media, for measurements of residual dipolar coupling (RDC), failed because of interference with halothane. It was found that the phage media coagulated upon halothane addition, and gel media gave a prohibitory fast relaxation in the presence of halothane. NMR experiments were performed at 25 °C on a 700 MHz spectrometer (Bruker Avance 700) equipped with a cryo-probe. Backbone and side-chain assignments were obtained using a combination of standard triple resonance experiments.[15] 2D HNHA, 3D HNCO, HNCA, HN(CO)CA, HNCACB and CBCA(CO)NH were used for the ^{1}H, ^{15}N and ^{13}C assignments of the protein backbone. Side-chains ^{1}H and ^{13}C assignments of the non-aromatic side chains were obtained using 3D HAHB(CO)NH, (H)CC(CO)NH, HCCH-COSY and HCCH-TOCSY spectra. Assignments were crosschecked for consistency with 3D ^{15}N-edited and ^{13}C-edited [^{1}H, ^{1}H]-NOESY spectra. The ^{1}H and ^{13}C spin systems of the aromatic side-chains where identified using 3D HCCH-COSY and HCCH-TOCSY spectra, while the sequential assignment was based on NOE connectivity in the ^{13}C-edited [^{1}H, ^{1}H]-NOESY spectrum. Methionine methyl-group ^{1}H and ^{13}C assignment was achieved using methionine-methyl $^{13}C_{\varepsilon}$-filtered [^{1}H–^{13}C]-HSQC spectrum and $^{13}C_{\gamma,\varepsilon}$-filtered [^{1}H–^{13}C]--HMBC spectrum.[15] NOESY spectra for structural constraints were recorded at mixing times of 50 ms, 100 ms and 150 ms. Quantitative J-correlation HNHA experiment[15] was used for

measurement of $^{3}J(H^{N}H^{\alpha})$ couplings. The $^{1}H–^{15}N$ heteronuclear NOEs[16] were recorded using a 500 MHz spectrometer (Bruker Avance 500). The multidimensional spectra were processed and analyzed in FELIX (Felix NMR, 2007). All analyses performed after peak picking (assignments and structural parameter calculations) were realized using custom programs in MATLAB (The MathWorks, 2007). About 1600 NOE distances (including 19 halothane–protein distances) where extracted (see Table I in Results) and applied with error limits deduced from values obtained at three mixing times. The backbone NOE contacts and $^{3}J(H^{N}H^{\alpha})$ couplings were in agreement with NMR solution structure of $[Ca^{2+}]_4$-CaM (1J7O & 1J7P[17]). Therefore, backbone dihedral angles of the free $[Ca^{2+}]_4$-CaM were used as constraints with an error limit of ±10°, except in few regions of missing experimental couplings or a larger chemical shift difference at the backbone between free and complexed CaM. In these regions (residues: 19–21, 38–43, 54–57, 63–67, 70–76, 92––95, 104–108, 144–147) error limits were increased to ±30°. All H-bonds of free $[Ca^{2+}]_4$-CaM were also enforced by the distance constraints. Additional distance constraints were defined to maintain coordination geometry around Ca^{2+}.

Structure calculations

The initial conformation of the $[Ca^{2+}]_4$-CaM N-terminus lobe (residues 1–76) or C-terminus lobe (82–148) was set to the most representative conformer of the reported NMR solution structure of $[Ca^{2+}]_4$-CaM, 1J7O.pdb or 1J7P.pdb, respectively.[17] Halothane was positioned ≈5 Å above the hydrophobic pocket of each terminus. QUANTA/XPLOR[18] was used for structure calculations: standard simulated annealing schedule, refinement by cooling and energy minimization with distance and dihedral restraints. The final structures were not sensitive to the initial positioning of halothane. Of the 50 structures produced (for each lobe), about 15 were within 10 % of the lowest energy structure. These low-energy structures were subjected to a short (100 steps steepest descend) energy minimization in the CHARMm22 force-field (Molecular Simulations Inc., 1994), without any restraints except that Ca^{2+} coordination geometry was kept fixed. Five structures (for each lobe) that fully complied with the constraints were selected in the final set.

Data deposition

The NMR constraints and atomic coordinates for the conformers were deposited at Protein Data Bank (PDB entries 2kug and 2kuh for N- and C- terminus lobes, respectively).

$[Ca^{2+}]_4$-CaM-skMLCKp binding

Binding was determined from the change in emission of the tryptophan residue in the skMLCKp peptide measured in a stirred narrow channel 1 cm fluorescence cuvette (Helman) using a Fluoromax-3 instrument (Jobin-Yvon-Spex). The excitation wavelength was 280 nm, the emission wavelength was 333 nm, the excitation and emission slit widths were 5 nm, and the integrated emission intensity was averaged from thirty 1 s scans. The assay buffer was 50 mM MOPS (pH 7.3), 100 mM KCl, 1 mM $MgCl_2$ and 0.1 mM $CaCl_2$. The solutions were filtered and centrifuged to remove light scattering interferants. A set of titration data were collected in the following order: the background emission from the buffer was measured first. Then 2.7 nM skMLCKp was added into the cuvette and the emission was remeasured. This solution was discarded and a fresh volume of buffer was added to a clean cuvette and the emission measured. Then $[Ca^{2+}]_4$-CaM was added to a concentration of 1.3 nM and the emission recorded. Finally, skMLCKp peptide was added to a concentration of 2.7 nM and the emission was recorded. The solution was discarded and the series of measurements was repeated for 2.7, 4.0, 8.0, and 16.0 nM concentrations of $[Ca^{2+}]_4$-CaM. There was minimal

variation in the baseline emission intensities between the samples. The emission intensity from the skMLCKp at each $[Ca^{2+}]_4$-CaM concentration was determined by subtracting the emission intensity of the sample of $[Ca^{2+}]_4$-CaM and buffer from the corresponding sample of $[Ca^{2+}]_4$-CaM, skMLCKp and buffer. The skMLCKp emission intensity was plotted as a function of $[Ca^{2+}]_4$-CaM concentration with error bars that represent the standard deviation of the thirty intensity values collected at 1 s intervals. Three sets of $[Ca^{2+}]_4$-CaM–skMLCKp titration data were collected and each was fitted with the following equation:

$$F = F_{\min} + F_{\max}\left[\frac{(CaM + skMLCK + K_d) - \sqrt{(CaM + skMLCK + K_d)^2 + 4CaM \times skMLCK}}{2skMLCK}\right]$$

where $F_{\min}$ is the emission intensity from 2.7 nM skMLCKp in the absence of $[Ca^{2+}]_4$-CaM, $F_{\max}$ is the emission intensity from 2.7 nM skMLCKp bound to $[Ca^{2+}]_4$-CaM, *CaM* is the concentration of $[Ca^{2+}]_4$-CaM, *skMLCKp* is the concentration of skMLCKp (fixed at 2.7 nM), and K_d is the dissociation constant.

The data fitting was realized using Origin 7.5 (OriginLab) and the parameters are reported as mean ± *sd* of the fits to the three-titration data sets.

$[Ca^{2+}]_4$-CaM-smMLCK activity

The $[Ca^{2+}]_4$-CaM-dependence of the smMLCK activity was measured using a spectroscopic method coupled to pyruvate kinase and lactate dehydrogenase,[19] which was modified to work in a 96-well format fluorescence plate reader. Briefly, when smMLCK transfers a phosphate group from ATP to MLC, it produces a molecule of ADP. Pyruvate kinase (PK) acts on ADP and phosphoenolpyruvate (PEP) to produce ATP and pyruvate. Lactate dehydrogenase (LDH) acts on pyruvate and NADH to produce NAD^+ and lactate. Thus, for each MLC phosphorylated, one molecule of the fluorescent NADH is converted to the non-fluorescent NAD^+. The specific activity of smMLCK was determined by recording the kinetics of NADH disappearance using a Fluostar Optima Fluorescence plate reader (BMG) with 350 and 460 nm excitation and emission filters, respectively. The kinetic assays were performed in triplicate on 200 µl samples. A typical well contained 20 mM MOPS (pH 7.5), 100 mM KCl, 0.1 mM EGTA, 1.5 mM dithiothreitol (DTT), 1.2 mM PEP, 10 µM NADH, 4.3 units of LDH/PK, 20 µM regulatory light chain (RLC), 100 ηg MLCK, and various amounts of $[Ca^{2+}]_4$-CaM. The maximum fluorescence intensity of the NADH in the wells was recorded prior to initiating the assay by automatically injecting 10 µl of a solution containing 6 mM ATP, 40 mM $MgCl_2$, and 10 mM $CaCl_2$, which dilute to a final concentration of 0.3 mM ATP, 2 mM $MgCl_2$, and 0.5 mM $CaCl_2$ in the wells. The time dependent decrease in NADH fluorescence was recorded at 30 s intervals for approximately 10 min, after which the reaction was stopped by automatically injecting 10 µl of 400 µM ADP (20 µM final concentration) into each well. The baseline fluorescence intensity of the NADH-depleted samples was then recorded.

RESULTS

Solution structure of $[Ca^{2+}]_4$-CaM–halothane complex

The aim was to determine the structure of the $[Ca^{2+}]_4$-CaM–halothane complex at low halothane concentrations, because physiological concentrations of a VA in anesthesia are rather low. The titration with halothane was followed by

NMR (Supplementary material to this paper) and saturation of the $[Ca^{2+}]_4$-CaM chemical shifts was established at about 1:30 CaM:halothane mole ratio. Significant changes were observed already at a 1:10 mole ratio, which was eventually selected as concentration at which the physiologically relevant CaM/halothane complex might be discernible.

Chemical shifts of the protein backbone in $[Ca^{2+}]_4$-CaM–halothane complex (at 1:10 mole ratio) differ in several regions from those of $[Ca^{2+}]_4$-CaM, measured in the absence of halothane (Fig. 1, bottom). The most pronounced differences were in the N-terminus. There were no significant differences in the region of the central linker (residues 77–82). The regional mobility of the complex, as probed by backbone $\{^1H\text{-}^{15}N\}$-NOE (Fig. 1, top), indicates that the central linker was mobile when halothane was bound. These findings signify that low-halothane complex of $[Ca^{2+}]_4$-CaM probably retains a flexible and distant disposition of the two Ca^{2+} binding domains, as was found in the NMR solution structure of $[Ca^{2+}]_4$-CaM.[17]

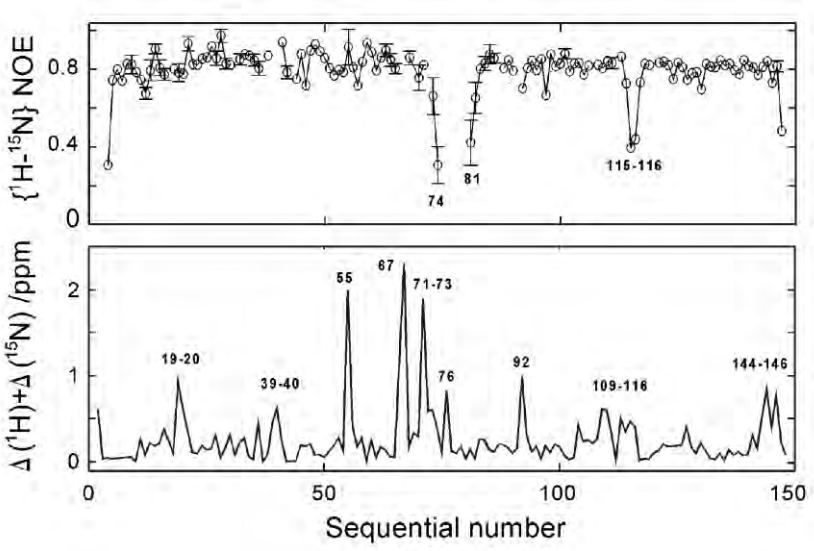

Fig. 1. Top: sequential values (open circles) of the backbone $\{^1H\text{-}^{15}N\}$-NOE; error bars are shown only when larger than the size of the open circles. Bottom: comparison of the CaM backbone chemical shift difference ($\Delta^1H = |\delta^1H_{complex} - \delta^1H_{free}|$, $\Delta^{15}N = |\delta^{15}N_{complex} - \delta^{15}N_{free}|$) between $[Ca^{2+}]_4$-CaM alone (free) and complexed with halothane.

A number of inter-molecular, $[Ca^{2+}]_4$-CaM to halothane NOE contacts were observed in each Ca^{2+} binding domain. All of them were between the single halothane proton and methyl-groups of CaM residues: Leu-32, Val-35, Met-36, Leu-39, Met-51, Val-55, Met-71, Met-72 and Met-76 in the N-terminus lobe, and

Leu-105, Val-108, Met-109, Leu-112, Met-124, Ala-128, Met-144 and Met-145 in the C-terminus lobe. The best quality NOE contacts were seen for the methyl groups of methionines because of their favorable relaxation properties (Fig. 2). Numerous intra-calmodulin NOE contacts (≈800 per lobe) were all in support of the lobe structures as found in the NMR solution structure of $[Ca^{2+}]_4$-CaM.[17]

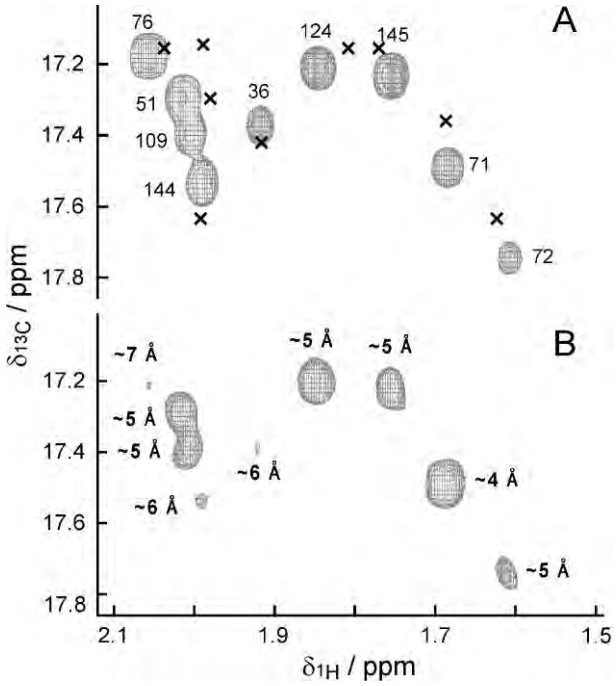

Fig. 2. Methyl-methionine ^{13}C-filtered 3D NOESY (200 ms mixing time) spectrum of $[Ca^{2+}]_4$-CaM–halothane complex. A) Diagonal peaks region (^1H region 1.5–2.1 ppm) of the spectrum. Peaks are labeled by sequential numbers of the methionines. The corresponding positions in halothane free $[Ca^{2+}]_4$-CaM[20] are marked by crosses. B) Halothane cross-peaks region (^1H region: 6.2–6.4 ppm) of the spectrum displayed peaks having centers at 6.3 ppm. Calculated methyl–halothane distances are shown.

The structure of the complex was solved under the assumption that halothane binding has a minor effect on the protein fold, which was justified by the similarity of the chemical shifts in $[Ca^{2+}]_4$-CaM determined with and without halothane, by the NOE contacts, and the $^3J(H^NH^\alpha)$ couplings. Thus, the protein dihedral angles (ψ, φ and χ^1) were constrained to those of free $[Ca^{2+}]_4$-CaM except in the regions of more pronounced (> 0.5 ppm) chemical shift differences (Fig. 1, bottom). Due to the flexible disposition of the two CaM lobes, the NMR solution structure was solved separately for the N-terminus and for the C-terminus lobes. The final structures were similar to the uncomplexed $[Ca^{2+}]_4$-CaM

structure[17] having an average deviation between the backbone or side-chains of ≈2 Å and ≈3 Å, respectively. The structural statistics are given in Table I.

The obtained structures (Fig. 3) show halothane binding in the region of the hydrophobic pockets, which are binding targets for many other ligands.[21] The N-terminus lobe structural models show a deeper imbedding of halothane than in the C-terminus, as could have been expected from the induced chemical shift changes of CaM (see above, Fig. 1, bottom). The orientation of the halothane varies considerably in the models, because there are no empirical constraints on the trifluoromethyl half of the molecule. An attempt was made to obtain additional constraints by measuring the $^{1}H–^{19}F$ dipolar couplings in oriented media, but halothane was found to disrupt the properties of the orientation media, *i.e.*, phage and co-solvents.

TABLE I. Summary of conformational restraints and structural statistics for 5 energy-refined conformers of $[Ca^{2+}]_4$-CaM in complex with halothane

Parameter	N-terminus	C-terminus
NOE distance restraints		
Intraresidual ($\|i–j\| = 0$)	314	337
Sequential ($\|i–j\| = 1$)	157	188
Medium range ($1 < \|i–j\| < 5$)	131	137
Long range ($\|i–j\| \geq 5$)	128+9[a]	137+10[a]
Total NOE	735	808
Dihedral angle restraints[b] (ψ, φ, χ^1)	220	195
H-bond restraints[b]	37	23
RMSD over all distance constraint violations, Å	0.1	0.1
RMSD over all dihedral angle restraints violations, deg.	2.5	3.2
CHARMm energies[c], kcal mol^{-1})		
Total	–2270±90	–1913±90
van der Waals	–316±9	–230±10
Electrostatic	–2285±90	–1970±100
Ramachandran plot statistics, %		
Residues in most favored region	90.3	95.7
Residues in additionally allowed regions	9.7	4.3
Residues in generously allowed regions	0	0
Residues in disallowed regions	0	0
Average *RMSD* from mean coordinates, Å		
All atoms	0.75	0.64

[a]Protein-halothane NOE; [b]target values are same as in $[Ca^{2+}]_4$-CaM structure (1J70 & 1P7O); [c]charged protein without Ca^{2+} counter-ions contribution

skMLCKp $[Ca^{2+}]_4$-CaM binding

The emission spectrum of the skMLCKp peptide excited at 280 nm was measured and it was found that the peak increased in intensity and was blue-shifted upon binding to $[Ca^{2+}]_4$-CaM (Fig. 4, top panel). This result is consistent

with previous.[22] The most significant difference between the spectra of the bound and unbound peptide was observed at 333 nm. The emission of the peptide at 333 nm at various $[Ca^{2+}]_4$-CaM concentrations up to 16 nM was measured (Fig. 4, bottom panel). The binding curves yielded a mean K_d of 1.3±0.4 nM, which agrees with the K_d value of 4 nM determined previously using surface plasmon resonance.[23] Moreover, 10 mM isoflurane did not significantly affect the fluorescence intensity of skMLCKp in the presence of 2.7 nM $[Ca^{2+}]_4$-CaM.

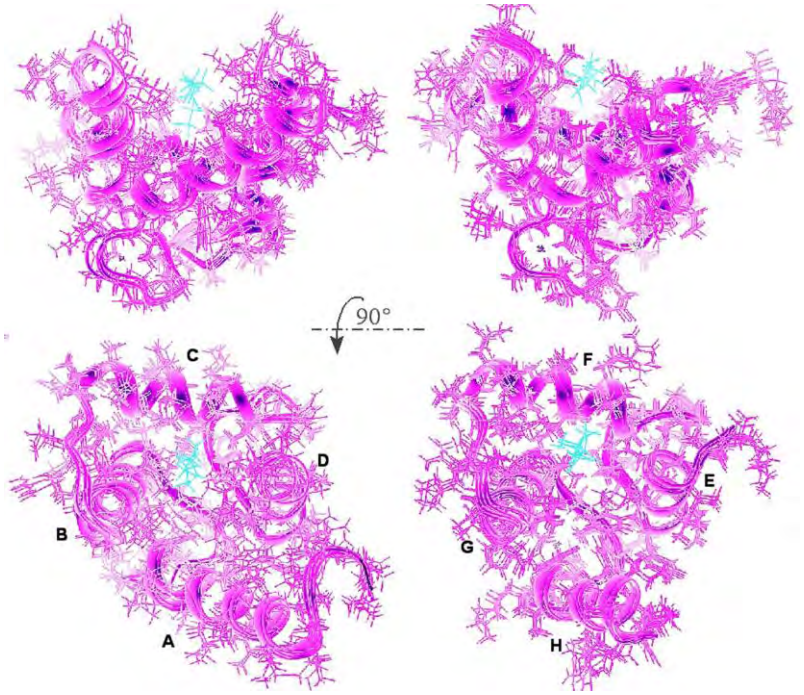

Fig. 3. Models of five conformers for N-terminus (to the left, 2KUG.pdb) and C-terminus (to the right, 2KUH.pdb) lobes of the $[Ca^{2+}]_4$-CaM–halothane complex. Halothane is given in cyan color, protein in magenda. The atomic stick-plot is overlain with protein cartoon (helices are denoted by letters).

smMLCK activity

The specific activity of smMLCK was determined using an ADP/NADH coupled assay. Representative spectra recorded in the presence of various concentrations of $[Ca^{2+}]_4$-CaM up to 300 nM illustrate the assay (Fig. 5, top panel). The initial plateau is the maximal emission from NADH, determined prior to initiating the assay. The drop in intensity (≈10 %) that occurred when a solution of ATP, $MgCl_2$, and $CaCl_2$ was automatically injected to start the reaction was due to minor ADP contamination. This was followed by a steady decrease in

NADH fluorescence that was dependent on the $[Ca^{2+}]_4$-CaM concentration. The rate of fluorescence decrease was directly proportional to the phosphorylation of the myosin light chain. The final steep drop occurred when an ADP solution was automatically injected, which consumes the remaining NADH. The end plateau was the signal from the sample without NADH. The difference between the plateaus at the beginning and end of the assay was used to calibrate the instrument response to the amount of NADH present.

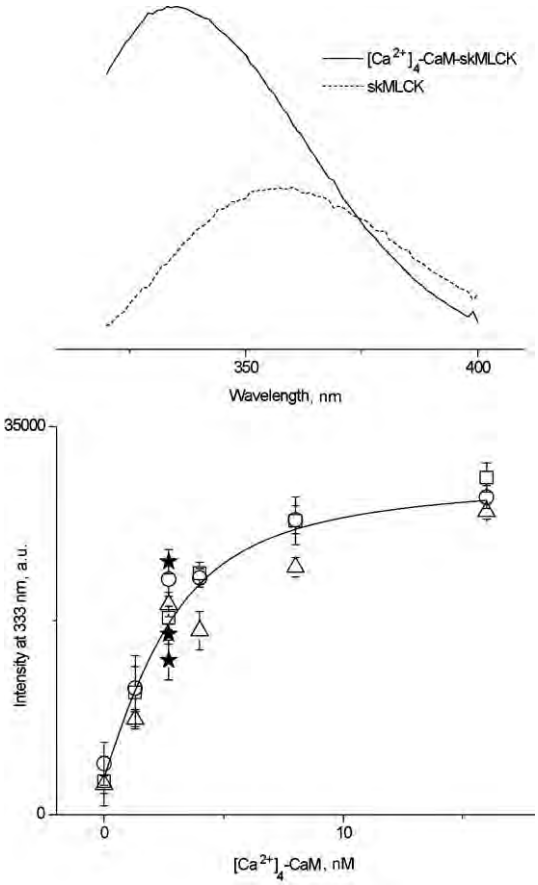

Fig. 4. Top: Change in tryptophan emission spectrum (at 280 nm) from skMLCKp upon binding to $[Ca^{2+}]_4$--CaM. Bottom $[Ca^{2+}]_4$-CaM concentration dependence of tryptophan emission (at 333 nm) from 2.7 nM skMLCKp. The titrations were repeated in triplicate (circles, squares and triangles). The error bars represent the standard deviation in the mean of thirty, 1 s fluorescence measurements. The solid line was generated using the mean parameters from the curve fits to the three sets of titration data. It was found that 10 mM isoflurane did not significantly affect the fluorescence intensity of skMLCKp in the presence of 2.7 nM $[Ca^{2+}]_4$-CaM (closed stars).

The specific activities of the smMLCK, calculated from the slopes are plotted as a function of $[Ca^{2+}]_4$-CaM concentration in Fig. 5, bottom panel. The maximum activity of smMLCK in the presence of $[Ca^{2+}]_4$-CaM was found to be approximately 12 μmol min^{-1} mg $MLCK^{-1}$, which is consistent with previous results.[19] The effect of various concentrations of halothane on the activity of MLCK alone and in the presence of $[Ca^{2+}]_4$-CaM at concentrations that produce half-maximal

(2 nM) and maximal (100 nM) activation was measured. Halothane was found to inhibit the MLCK activity, but it was not $[Ca^{2+}]_4$-CaM dependent (Fig. 6).

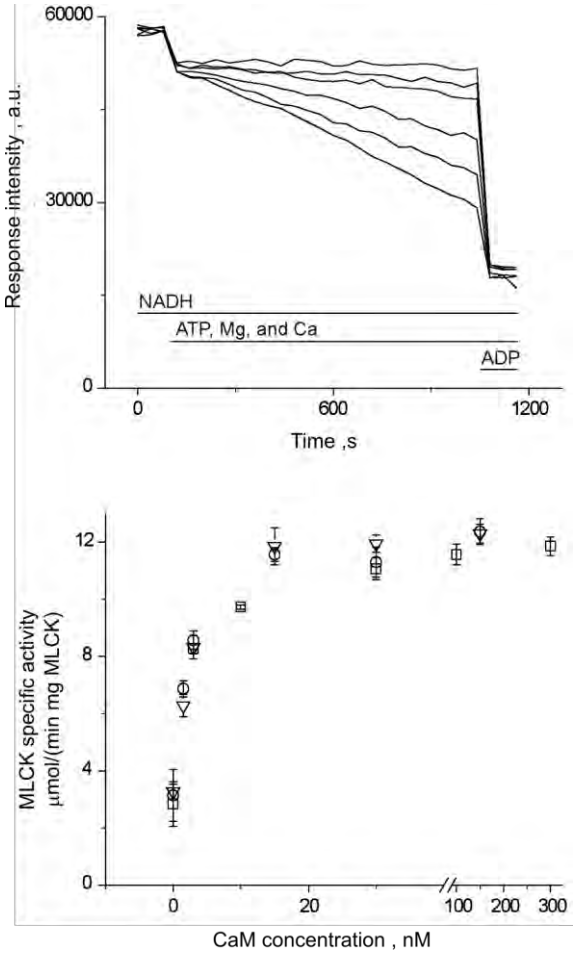

Fig. 5. Top: raw fluorescence data for assay of CaM-dependent MLCK activity. From top to bottom trace, CaM concentration was 0, 1, 3, 10, 30, and 100 nM. Bottom: $[Ca^{2+}]_4$--CaM dependence of MLCK specific activity.

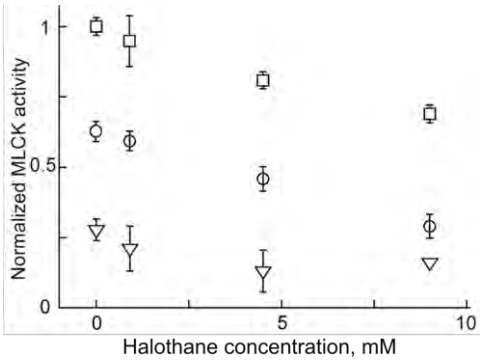

Fig. 6. Effect of halothane on MLCK activity. The activities were measured in the presence of 0, 2 and 100 nM concentrations of $[Ca^{2+}]_4$-CaM, indicated by the triangle, circle and square symbols, respectively. The activities are normalized to the specific activity of MLCK measured in the presence of 100 nM $[Ca^{2+}]_4$-CaM without halothane. Increasing concentrations of halothane inhibited MLCK, independent of the $[Ca^{2+}]_4$--CaM concentration.

DISCUSSION

Halothane binding site

The NMR solution structure of the $[Ca^{2+}]_4$-CaM–halothane complex appears to retain an open structure with a flexible central-linker, which is consistent with free $[Ca^{2+}]_4$-CaM. Therefore, halothane binding does not seem to induce a global conformational change in the $[Ca^{2+}]_4$-CaM structure. To gain insight into the structural features of halothane binding, its binding is compared in Fig. 7 with that of a potent CaM-peptide binding antagonist *N*-(6-aminohexyl)-5-chloro-1-naphthalenesulfonamide (W-7).[24] Halothane does not penetrate as deep into the hydrophobic pockets in the termini of $[Ca^{2+}]_4$-CaM as does W-7. Halothane mainly

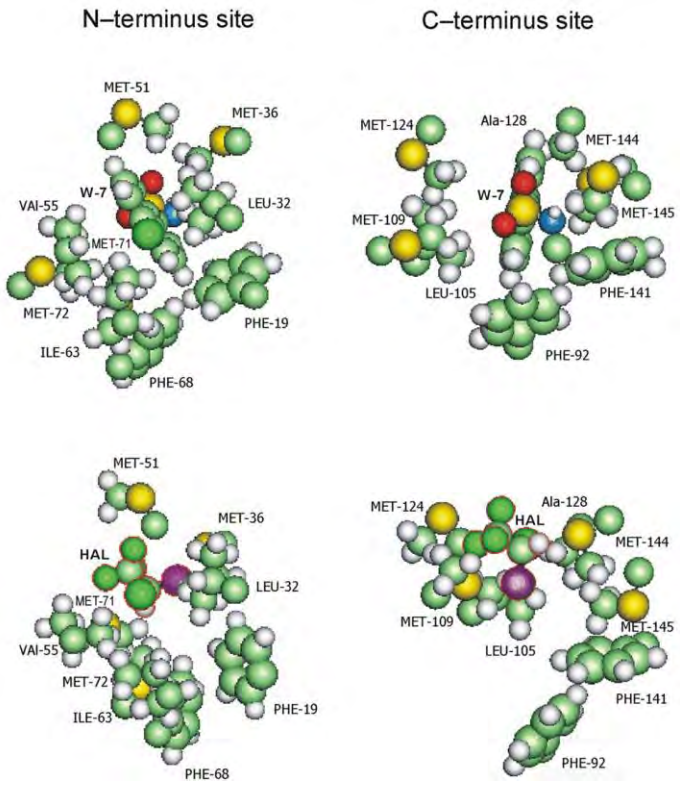

Fig. 7. Top: partial structure of the binding sites of *N*-(6-aminohexyl)-5-chloro-1-naphthalenesulfonamide (W-7) to $[Ca^{2+}]_4$-CaM (taken from 1mux.pdb, first NMR structure). Shown are the side-chain groups of $[Ca^{2+}]_4$-CaM binding sites in contact with the W-7 aromatic ring. Bottom: analogous view of the binding site in the $[Ca^{2+}]_4$-CaM–halothane structure. The structure of the conformer with a deepest imbedding of halothane is shown. Atoms are represented by solid spheres at 50 % of the van der Walls radii. Colors are by atom nature: H (white-gray), C (light green), N (blue), O (red), F (deep-green), S (yellow), Cl (deep-green), Br (magenta).

interacts with methyl groups, primarily from methionine residues, whereas W-7 also interacts with complementary aromatic groups at the base of the pockets. This preferential interaction with methyl groups is likely supported by their high concentration at the pockets entry. In a more dominant aromatic environment, halothane could also engage aromatic groups.[25] The lack of halothane penetration into the C-terminal pocket is particularly significant because that is where the tryptophan side chains (*i.e.*, Trp-4 of the CaM-binding peptide from the MLCK,[24] or Trp-8 of the CaM-binding peptide[26,27]) anchor the peptide to $[Ca^{2+}]_4$-CaM.

To substantiate further this finding, comparison of the ligand penetration depth into the hydrophobic pockets of $[Ca^{2+}]_4$-CaM by triangulation to three residues at the bottom of the pockets that are iso-topical in the N- and C-terminuses was made (Scheme 1 and Table II). The data in the last two columns of Table II verify that ligand penetration depth into the C-terminus hydrophobic pocket is crucial for the onset of antagonist behavior.

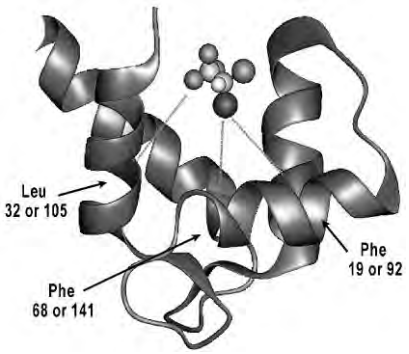

Scheme 1. Ligand penetration into the hydrophobic pockets of $[Ca^{2+}]_4$-CaM.

TABLE II. Ligand penetration-depths into hydrophobic pockets of Ligand/CaM (Ligand/#pdb) structures obtained by triangulation to three residues at the bottom of the hydrophobic pockets. Distances (Å) were calculated between the backbone C^{α} atom of the three residues and the closest heavy atom of the ligand; TFP: 10-[3-(4-methyl-piperazin-1-yl)--propyl]-2-trifluoromethyl-10*H*-phenothiazine

Ligand/#pdb	Phe19	Leu32	Phe68	Mean	Phe92	Leu105	Phe141	Mean	Antagonist
EtOH	C1:	C1:	C2:	–	Any	Any	Any	–	–
/1cll	8.1	7.5	5.9	**5.6**	>15	>15	>15	**>15**	No
Halothane	Br:	Cl2:	Br:	–	C1:	Cl2:	F2:	–	–
/2kug, 2kuh	11.5	8.2	7.6	**9.1**	13.1	7.3	8.3	**9.6**	No
W-7	C3:	C4:	C3:	–	C3:	C3:	Cl1:	–	–
/1mxu	6.4	6.6	7.2	**6.7**	6.1	6.4	6.4	**6.3**	Yes
TFP	C3:	C3:	C2:	–	C9:	C9:	C10:	–	–
/1ctr	13.6	17.3	15.2	**15.4**	7.6	5.8	6.5	**6.6**	Yes
MLCK	10CB:	14CD1:	17CD2:	–	8O1:	8O1:	4CZ2:	–	–
/1qs7	7.0	6.9	7.4	**7.1**	5.3	5.7	5.5	**5.5**	Yes

The finding that halothane interacts with methyl groups in $[Ca^{2+}]_4$-CaM is consistent with previous observations that VAs contact primarily aliphatic residues in serum albumin[28] and interact solely with the choline methyl groups in dipalmitoylphosphatidylcholine vesicles.[29] This appears to be a general feature of VAs–protein interactions, which were used as criteria to identify amphiphilic pockets in protein structures where VAs bind.[10,11] This finding is consistent with the possibility that protein methyl groups act as weak hydrogen bond donors to the methyl halogens, namely fluorine, found in VAs.[30] However, this is only speculation because data necessary for the determination of the orientation of halothane relative to the methyl groups of $[Ca^{2+}]_4$-CaM is lacking.

Isoflurane does not affect steady-state $[Ca^{2+}]_4$-CaM–skMLCKp binding

The steady state fluorescence assay indicated that even high concentrations of isoflurane and, by extension, probably other VAs, do not significantly alter the amount of $[Ca^{2+}]_4$-CaM–skMLCKp formed in the presence of 2.7 nM $[Ca^{2+}]_4$--CaM. Isoflurane was used because it does not quench fluorescence unlike halothane, which would complicate the interpretation of this assay, and skMLCKp was employed because its affinity for $[Ca^{2+}]_4$-CaM is not too high to quantify.[23] Thus VAs do not behave like the $[Ca^{2+}]_4$-CaM antagonist W-7, which reduces the amount of $[Ca^{2+}]_4$-CaM–MLCK peptide formed without significantly altering the K_d value.[31] This was unexpected since halothane was shown to reduce the amount of synaptic PDZ domain-mediated protein interactions with NMDA receptor and nNOS without significantly altering the K_d value.[32] It is possible that VAs behave like the $[Ca^{2+}]_4$-CaM antagonist TFP and alter the on-rate of the MLCK peptide, but not the steady state amount of complex formed.[31] However, a reduction in the on-rate would increase the steady state K_d and right-shift the binding curve. This was not the case since isoflurane had no effect on the intensity observed near the half-maximal $[Ca^{2+}]_4$-CaM. These results indicate that VAs do not significantly antagonize the interaction of $[Ca^{2+}]_4$-CaM with skMLCKp.

Halothane inhibits smMLCK activity

The kinetic fluorescence assay indicated that the MLCK activity is inhibited in a concentration-dependent manner by halothane. Fluorescence quenching by halothane does not present a problem for this assay because the instrument response is calibrated using the NADH fluorescence from each sample condition. It was found that MLCK is inhibited by VAs in the absence of $[Ca^{2+}]_4$-CaM and in the presence of sub-maximal and maximal concentrations of $[Ca^{2+}]_4$-CaM. This indicates that the mechanism by which halothane inhibits MLCK is independent of $[Ca^{2+}]_4$-CaM, which is consistent with the finding that isoflurane does not inhibit $[Ca^{2+}]_4$-CaM binding to skMLCKp.

CONCLUSIONS

The obtained results indicate that VAs bind to antagonist sites in $[Ca^{2+}]_4$--CaM, yet inhibit MLCK activity only *via* unspecified interactions with the enzyme. The inability of VAs to act as potent CaM-peptide binding antagonists can be traced to the ligand-penetration-depth into the C-terminus hydrophobic pockets. The result is significant because it shows, at least in the case of calmodulin-dependent smMLCK activity, that effect of VAs on enzyme function do not arise from the low affinity of VA binding to the druggable sites of the protein.

Since mechanism of general anesthesia remains unsolved,[33] structural studies at an atomic resolution level, such as those presented herein, could help understand modalities of anesthetic–biomacromolecule interactions.

SUPPLEMENTARY MATERIAL

Two figures presenting halothane/CaM NMR titration data are available electronically at http://www.shd.org.rs/JSCS/ or at: https://www.researchgate.net/profile/Nenad_Juranic/publications/?pubType=dataset&ev=prf_pubs_dat

Acknowledgment. This study was supported in part by grants GM070585 and HL-45532 from the National Institutes of Health, Bethesda, Maryland, USA.

ИЗВОД

ХАЛОТАН СЕ ВЕЗУЈЕ ЗА АКТИВНА МЕСТА $[Ca^{2+}]_4$-КАЛМОДУЛИН, АЛИ НЕ ИНХБИРА $[Ca^{2+}]_4$-КАЛМОДУЛИН-ЗАВИСНУ АКТИВАЦИЈУ КИНАЗЕ

NENAD O. JURANIĆ[1], KEITH A. JONES[2], ALAN R. PENHEITER[1], THOMAS J. HOCK[2] и JOHN H. STREIFF[2]

[1]*Mayo College of Medicine at Rochester, U.S.A. и* [2]*University of Alabama at Birmingham, U.S.A.*

Механизам деловања испарљивих анестетика је слабо познат. Применом NMR спектроскопије виоске резолуције ми смо решили структуру комплекса којег испарљиви анестетик халотан чини са калцијум-везујућим протеином калмодулином ($[Ca^{2+}]_4$--CaM). Утврдили смо да се халотан везује за калмодулин на местима која су позната као примарна места везивања разних лиганада, и сматрају се примарним циљем за примену лекова у системима зависним о сигнализирању калцијума. То је указивало на могућност дејства анестетика путем модулације сигнализирања калцијум-кадмодулина. Зато смо испитали да ли везивање испарљивих анестетика (VA) утиче на калцијум-кадмодулин зависну активност ензима миозин-киназе (*myosin light chain kinase*, MLCK). Применом флуоресцентне анализе утврдили смо да VA утичу на активацију MLCK, али да не мења константу везивања калцијум-калмодулина за моделну регију ензима (skMLCKp). Овај резултат сугерише да анестетик (VA) не утиче директно путем сигнализирања калцијум--кадмодулина.

(Примљено 23. маја 2013)

REFERENCES

1. N. P. Franks, E. R. Lieb, *Nature* **310** (1984) 599
2. M. Zhang, T. Tanaka, M. Ikura, *Nat. Struct. Biol.* **2** (1995) 758

3. L. J. Van Eldick, D. M. Watterson, *Calmodulin and Signal Transduction:An Introduction*, in *Calmodulin and Signal Transduction*, L. J. Van Eldik, D. M. Watterson, Eds., Academic Press, New York, USA, 1998, p. 1
4. W. J. Cook, L. J. Walter, M. R. Walter, *Biochemistry* **33** (1994) 15259
5. L. Massom, H. Lee, H. W. Jarett, *Biochemistry* **29** (1990) 671
6. F. Orosz, T. Y. Christova, J. Ovadi, *Mol. Pharmacol*. **33** (1988) 678
7. R. Chattopadhyaya, W. E. Meador, A. R. Means, F. A. Quiocho, *J. Mol. Biol.* **228** (1992) 1177
8. L. Ohashi, R. Pohoreki, K. Morita, P. M. Stemmer, *Biochim. Biophys. Acta, Mol. Cell Res*. **1691** (2004) 161
9. A. Levin, T. J. J. Blanck, *Anesthesiology* **83** (1995) 120
10. J. H. Streiff, T. W. Allen, E. Atanasova, N. Juranic, S. Macura, A. R. Penheiter, K. A. Jones, *Biophys. J*. **91** (2006) 3405
11. J. H. Streiff, K. A. Jones, *J. Chem. Inf. Model*. **48** (2008) 2066
12. J. Marley, M. Lu, C. Bracken, *J. Biomol. NMR* **20** (2001) 71
13. J. A. Putkey, G. R. Slaughter, A. R. Means, *J. Biol. Chem.* **260** (1985) 4704
14. K. Ajtai, M. F. Halstead, M. Nyitrai, A. R. Phenheiter, Y. Zheng, T. P. Burghardt, *Biochemistry* **48** (2009) 5263
15. A. Bax, *Curr. Opin. Struct. Biol*. **4** (1994) 738
16. S. Grzesiek, A. Bax, *J. Am. Chem. Soc.* **115** (1993) 12593
17. J. J. Chou, S. P. Li, C. B. Klee, A. Bax, *Nat. Struct. Biol.* **8** (2001) 990
18. A. T. Brunger, *X-PLOR Version 3.1: A System for X-ray Crystallography and NMR*, Yale University, New Haven, CT, 1992
19. K. Torok, D. J. Cowley, B. D. Brandmeier, S. Howell, A. Aitken, D. R. Trentham, *Biochemistry* **37** (1998) 6188
20. M. Ikura, L. E. Kay, A. Bax, *Biochemistry* **29** (1990) 4659
21. S. W. Vetter, E. Leclerc, *Eur. J. Biochem*. **270** (2003) 404
22. A. M. Weljie, H. J. Vogel, *Protein Eng.* **13** (2000) 59
23. S. Montigiani, G. Neri, P. Neri, D. Neri, *J. Mol. Biol.* **258** (1996) 6
24. M. Osawa, M. B. Swindells, J. Tanikawa, T. Tanaka, T. Mase, T. Furuya, M. Ikura, *J. Mol. Biol.* **276** (1998) 165
25. T. Cui, V. Bondarenko, D. Ma, C. Canlas, N. R. Brandon, J. S. Johansson, Y. Xu, P. Tang, *Biophys. J*. **94** (2008) 4464
26. B. Elshorst, M. Hennig, H. Forsterling, A. Diener, M. Maurer, P. Schulte, H. Schwalbe, C. Griesinger, J. Krebs, H. Schmid, T. Vorherr, E. Carafoli, *Biochemistry* **38** (1999) 12320
27. N. Juranic, E. Atanasova, A. G. Filoteo, S. Macura, F. G. Prendergast, J. T. Penniston, E. E. Strehler, *J. Biol. Chem.* **285** (2010) 4015
28. K. Shikii, S. Sakurai, H. Utsumi, H. Seki, M. Tashiro, *Anal. Sci*. **20** (2004) 1475
29. S. Yokono, K. Ogli, S. Miura, I. Ueda, *Biochim. Biophys. Acta* **982** (1989) 300
30. E. Kryachko, S. Scheiner, *J. Phys. Chem., A* **108** (2004) 2527
31. K. Sasaki, T. Ozawa, Y. Umezawa, *Anal. Chim. Acta* **447** (2001) 63
32. M. Fang, Y. X. Tao, F. H. He, M. J. Zhang, C. F. Levine, P. Z. Mao, F. Tao, C. L. Chou, S. Sadegh-Nasseri, R. A. Johns, *J. Biol. Chem.* **278** (2003) 36669
33. P. L. Chau, *Br. J. Pharmacol*. **161** (2010) 288.